Chemical Engineering Journal 91 (2003) 235–242

www.elsevier.com/locate/cej

# Ammonia oxidation into nitrous oxide over Mn/Bi/Al catalyst
## I. Single cooling tube experiments

A.S. Noskov, I.A. Zolotarskii, S.A. Pokrovskaya*, V.N. Korotkikh,
E.M. Slavinskaya, V.V. Mokrinskii, V.N. Kashkin

*Boreskov Institute of Catalysis, pr. Akademika Lavrentieva, 5 Novosibirsk, Russia*

## Abstract

The process of ammonia oxidation with air oxygen was tested on the pilot-scale using a single-tube reactor to model the unit of a multi-tubular industrial reactor. The spherical Mn/Bi/Al catalyst was loaded into the reactor tube. Experimental studies were based on the data obtained by kinetic studies and simulation of the tubular reactor. The relationship between the operation conditions and temperature regime was established by varying the process parameters over a wide range. The steady-state temperature regimes were observed at the inlet ammonia concentration equal to 4–5%. The selectivities to nitrous oxide and nitrogen oxide reached 87–88% and no more than 0.5%, respectively, at near 100% conversion of ammonia.

Modeling of the pilot reactor demonstrated a good agreement between the experimental and calculated data that supports appropriateness of the reactor simulation for prediction of technological regimes for the industrial reactor. The Rashig rings loaded in the tubular reactor were found to provide stable operation regimes at the inlet ammonia concentration of 7–8%.

*Keywords:* Mn/Bi/Al catalyst; Ammonia oxidation; Nitrous oxide; Pilot testing; Tubular reactor

## 1. Introduction

In the recent years, nitrous oxide has become used as a mild oxidizer for partial oxidation of hydrocarbons, for example oxidation of benzene to phenol. A new one-stage technology for production of phenol from benzene (AlphOx process) was developed by the Boreskov Institute of Catalysis (BIC) in cooperation with Solutia Inc. [1–3]. The new hydroxylation technology was initially developed as an integral part of the new process for production of adipic acid using waste nitrous oxide but then competitiveness of the AlphOx process with nitrous oxide obtained by oxidation of ammonia was demonstrated [3].

The strong appeal of the $N_2O$-based partial oxidation promotes search for inexpensive feedstocks. That is why, the process for direct ammonia oxidation is of interest to numerous researchers [4–6]. Solutia Inc. and BIC are engaged in the project on ammonia oxidation into nitrous oxide to be used as a feedstock for production of phenol from benzene. Some of the results obtained under this project are discussed in the present paper.

The aim of this study is to accomplish pilot testing of the reaction of ammonia oxidation over a proprietary Mn/Bi/Al catalyst using a single cooling tube as the model of a unit of the industrial multi-tubular reactor and to check if the used mathematical description is appropriate for prognosis of the technological regimes. We address here lab-scale kinetics studies, reactor modeling and pilot-scale trials of this process.

## 2. Catalyst

Several systems are known to catalyze selective oxidation of ammonia by oxygen to yield nitrous oxide [5–7]. Mn and Bi oxide catalysts supported on alumina [8] were developed for this process at the Boreskov Institute of Catalysis. The catalysts were prepared by impregnating alumina spheres with solutions of manganese and bismuth nitrates, drying and calcination at 375–550 °C. Prepared catalysts contained 35–90% of alumina at the specific surface area equal to 5–80 $m^2$/g. A high catalytic activity even with reaction mixtures containing oxygen in substoichiometric amount, a high selectivity to nitrous oxide at a low selectivity to nitrogen oxide was characteristic of these catalysts over a wide temperature range.

---

* Corresponding author. Tel.: +7-3832-341278/344491; fax: +7-3832-341878.
*E-mail address:* pokrov@catalysis.nsk.su (S.A. Pokrovskaya).

1385-8947/02/$ – see front matter © 2002 Elsevier Science B.V. All rights reserved.
PII: S1385-8947(02)00159-6

**Nomenclature**

| | |
|---|---|
| $A_D$, $A_\lambda$, $A_\alpha$ | constant parameters of relationships for mass and heat transfer parameters |
| $B_D$, $B_\lambda$, $B_\alpha$ | constant parameters in the same place |
| $C_0$, $C$ | inlet and current ammonia concentrations, correspondingly (mol/mol) |
| $C_\mathrm{p}$ | specific heat capacity (J/(mol/K)) |
| $D_\mathrm{g}$ | molecular diffusivity ($m^2$/s) |
| $D_\mathrm{r}$ | effective radial diffusivity ($m^2$/s) |
| $l$ | current reactor height (m) |
| $L$ | total reactor height (m) |
| $Pr$ | Prandtl number |
| $r$ | current reactor tube radius (m) |
| $R$ | effective reactor tube radius (m) |
| $Re$ | Reynolds number |
| $Q$ | heat release of reaction (J/mol) |
| $Sc$ | Schmidt number |
| $T$ | catalyst temperature (K) |
| $T_\mathrm{c}$ | cooling agent temperature (K) |
| $T_0$ | gas mixture temperature at reactor inlet (K) |
| $u$ | superficial gas velocity (m/s) |
| $W$ | total ammonia conversion rate (mol/($m^3$ s)) |

*Greek letters*

| | |
|---|---|
| $\alpha_\mathrm{w}$ | wall heat transfer coefficient (J/($m^2$/s/K)) |
| $\lambda_\mathrm{g}$ | thermal conductivity (J/(m s K)) |
| $\lambda_\mathrm{r}$ | effective radial thermal conductivity (J/(m s K)) |

Pilot testing was carried out using batches of spherical catalyst (3–6 mm spheres). Samples to be used for the kinetic studies were crushed to obtain 0.25–0.5 mm fraction.

## 3. Kinetic studies

Laboratory studies of catalytic properties were performed using a continuous tank reactor under stirring and an isothermal plug reactor by varying reaction conditions (Table 1).

The influence of temperature, contact time and inlet reactant concentrations were studied. The aim was to choose conditions providing the minimal rate of formation of side products and the highest selectivity to $N_2O$.

Table 1
Reaction conditions

| | |
|---|---|
| Catalyst weight (g) | 0.05–4 |
| Temperature (°C) | 270–400 |
| Pressure (bar) | 1–3 |
| Contact time (s) | 0.03–12 |
| Inlet reagent concentrations (vol.%) | |
| Ammonia | 0.75–12 |
| Oxygen | 1.5–14 |
| Water | 0–43 |

The catalyst performance was compared for the cases of deficient and excess oxygen. The studies revealed that oxygen and nitrous oxide were competitive oxidants of ammonia. Oxygen being a stronger oxidant, the interaction of $N_2O$ with ammonia was insignificant at excess oxygen at temperatures below 370 °C. Again, the excess oxygen decelerated the reaction of $N_2O$ decomposition. The catalyst behavior also was studied with NO added to the inlet mixture. Competitive reactions of NO reduction with ammonia and oxidation of ammonia were observed. The rate of ammonia oxidation was higher than that of NO reduction at above 300 °C so that consumption of ammonia was higher than consumption of NO. At 270–300 °C, the rate of ammonia oxidation but not the rate of NO reduction decreased sharply.

The main reactions proceeding on the catalyst surface under the optimal process conditions were supposed based on the results obtained and these stoichiometric pathways were further used as the basis of linearly independent chemical equations [9]:

$$\begin{aligned} 2NH_3 + 2O_2 &= N_2O + 3H_2O \\ 4NH_3 + 3O_2 &= 2N_2 + 6H_2O \\ 4NH_3 + 5O_2 &= 4NO + 6H_2O \end{aligned} \tag{1}$$

The activation energies were estimated for formation of nitrous oxide, nitrogen and nitrogen oxide. For nitrous oxide, it was found to be higher than that for nitrogen but lower than that for nitrogen oxide. Therefore, the optimal temperature range can be chosen for achieving the maximal selectivity to $N_2O$ (Fig. 1). This range depends on the concentration of reagents in the system. An increase in the concentration of oxygen and water leads to an increase in the selectivity to $N_2O$ (see Fig. 2 for an example). The range of the reaction conditions was determined where the selectivity to nitrous oxide reaches 90–92% while the selectivity to nitrogen oxide remains as low as 0.3–0.5%.

## 4. Reactor modeling

The main goal of these studies was to determine the optimal dimensions and operating conditions of tubular reactor allowing to realize the process with the maximal possible catalyst productivity to $N_2O$. Modeling procedure included:

- modeling of temperature profiles in a tubular reactor with a spherical catalyst;
- determination of parameters and test conditions for the pilot reactor;
- evaluation and correction of heat transfer coefficients for pilot set-up using special experiments with air and air/steam fed to the inlet of catalyst bed reactor;
- simulation of pilot operation regimes and comparison of experimental and calculated data;
- modeling of temperature profiles in the tubular reactor with a Rashig ring catalyst.

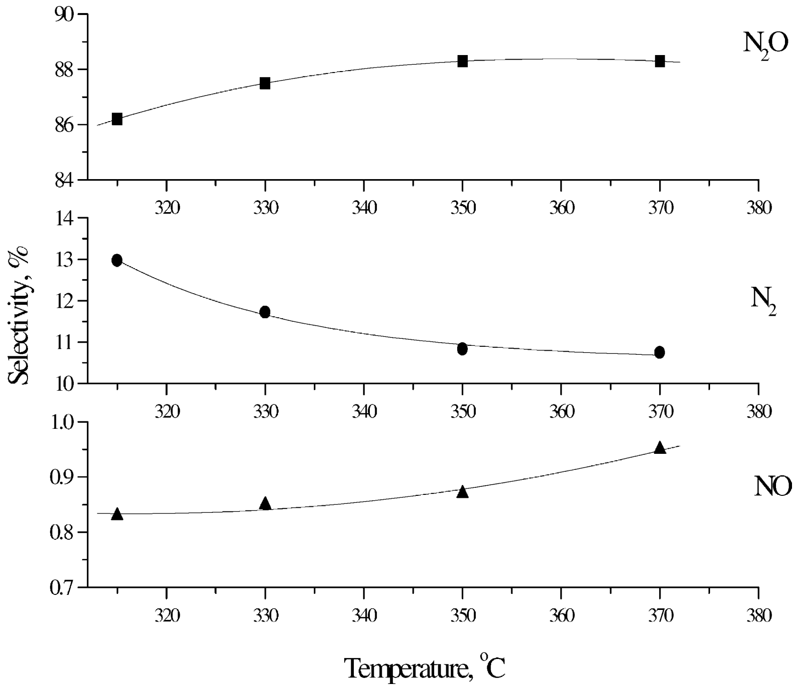

Fig. 1. Temperature effect on product selectivities. Inlet ammonia concentration is 7 vol.%, inlet oxygen concentration is 8 vol.%.

The commonly known quasi-homogeneous model accounting for the heat and mass transfer along the tube radius was used to estimate reactor parameters under stationary conditions

$$D_{\mathrm{r}}\left(\frac{\partial^2 C}{\partial r^2}+\frac{1}{r}\frac{\partial C}{\partial r}\right)-u\frac{\partial C}{\partial r}-W=0,$$

$$\lambda_{\mathrm{r}}\left(\frac{\partial^2 T}{\partial r^2}+\frac{1}{r}\frac{\partial T}{\partial r}\right)-uC_{\mathrm{p}}\frac{\partial T}{\partial l}+QW=0 \qquad (2)$$

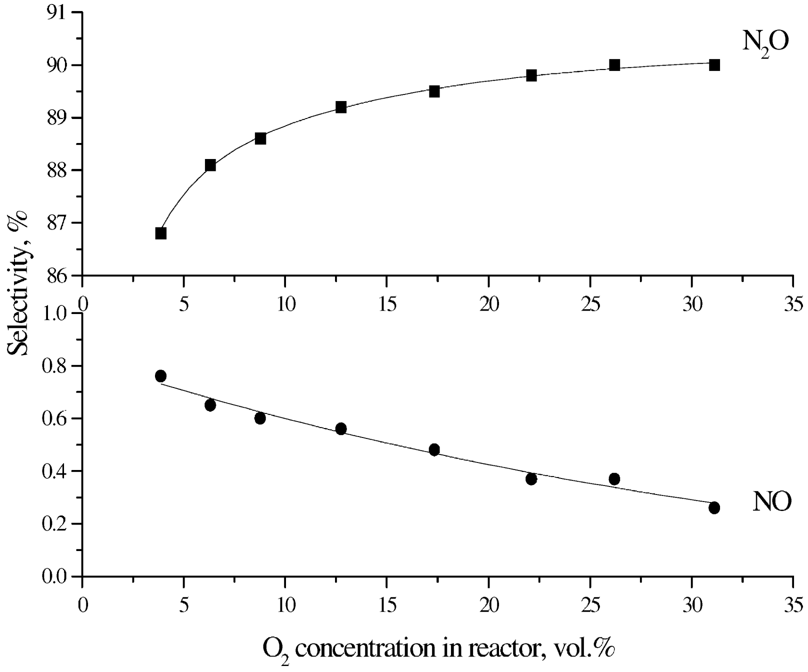

Fig. 2. $N_2O$ selectivity vs. oxygen concentration at temperature 350 °C and inlet ammonia concentration is 7 vol.%.

where the boundary conditions are:

$$\begin{array}{lll} l=0, & C=C_0, & T=T_0 \\ r=0, & \dfrac{\partial C}{\partial r}=0, & \dfrac{\partial T}{\partial r}=0 \\ r=R, & \dfrac{\partial C}{\partial r}=0, & \lambda_r \dfrac{\partial T}{\partial r}=\alpha_w(T_c-T) \end{array}$$

The following simplifications were used: (1) reaction selectivity was constant; (2) first-order equations were valid for product formation rates; (3) gas pressure was invariable along the tube length; (4) the cooling agent temperature was not varied along the tube length; (5) catalyst effectiveness factor was constant. The description of reaction rate $W$ and reaction heat release $Q$ expressions could be found in Appendix A.

Evaluation of mass and heat transfer parameters was made using conventional relationships with static and dynamic contributions [10,11], namely:

$$\frac{D_r}{D_g}=A_D+B_D Re\,Sc;$$
$$\frac{\lambda_r}{\lambda_g}=A_\lambda+B_\lambda Re\,Pr; \quad Nu=A_\alpha+B_\alpha Re^{0.8}Pr^{0.33} \qquad (3)$$

To choose optimal operation regimes for the pilot reactor the restrictions were imposed:

1. Hot spot catalyst temperature is not higher than 400 °C to avoid $N_2O$ selectivity losses.
2. Hot spot temperature sensitivity to cooling agent temperature (HSCA) defined as an increase in hot spot temperature with cooling agent temperature rise by 1 °C is not higher than 4.0 for spherical catalyst particles and than 5.0 for the ring catalyst.
3. Pressure drop along the reactor tube is not higher than 0.8 bar.

The following parameters were varied: inlet concentrations of ammonia, oxygen and steam, tube diameter, superficial gas velocity, cooling agent temperature, inlet gas mixture temperature, catalyst activity and particle diameter. It was shown that control parameters that mainly affect the reactor performance at a constant tube diameter were superficial gas velocity, temperature of the cooling agent and the inlet ammonia concentration. The inlet gas temperature influences only slightly the reactor operation mode; the temperature range was chosen based on the following speculations: the temperature at the reactor inlet must allow the inlet gas to be heated in the recuperative heat exchanger but not nitrate salts to be formed. Modeling enabled to determine optimal dimensions of the pilot reactor, to choose optimal operation regimes for pilot testing and to find an appropriate catalyst activity.

Optimal reactor parameters and test conditions calculated are given in Table 2. All the operation regimes are in accordance with restrictions 1–3 given earlier.

Table 2
Pilot reactor parameters and test conditions

| | |
|---|---|
| Catalyst height (m) | 1.5–4 |
| Tube diameter (cm) | 2.5–3.5 |
| Catalyst particle diameter (mm) | 3–6 |
| Catalyst load (l) | 0.8–3.5 |
| Gas superficial velocity (St m/s) | 2–3.5 |
| Inlet gas composition (vol.%) | |
| Ammonia | 3–5 |
| Water | 0–20 |
| Air | Balance |
| Catalyst temperature (°C) | 230–400 |
| Average pressure (bar) | 1.5–2.5 |

## 5. Pilot reactor testing

### 5.1. Design of the pilot reactor

Synthesis of nitrous oxide by partial oxidation of ammonia with air oxygen in the presence of steam was studied using a single-tube reactor to model the unit of a multi-tubular industrial reactor. Fig. 3 illustrates the reactor set-up. The catalytic reactor consisted of a 28 mm i.d. U-like tube with loaded catalyst granules and two 6 mm o.d. vertical tubes

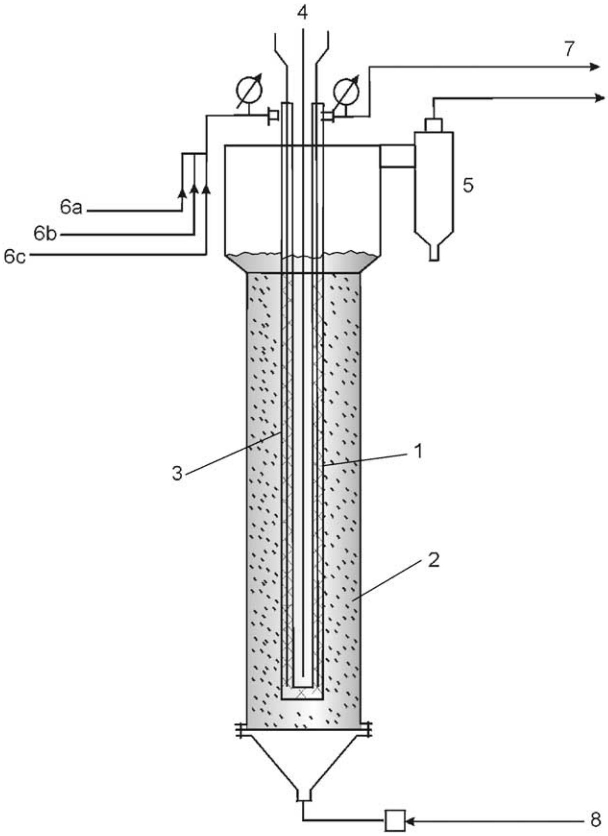

Fig. 3. Pilot installation: (1) reactor tube; (2) thermostat; (3) catalyst loading; (4) thermocouples in reactor tube and fluidized bed; (5) cyclone; (6a–c) feed of preheated ammonia, air and steam; (7) reaction mixture outlet; (8) hot air feed for fluidization; (9) air from thermostat.

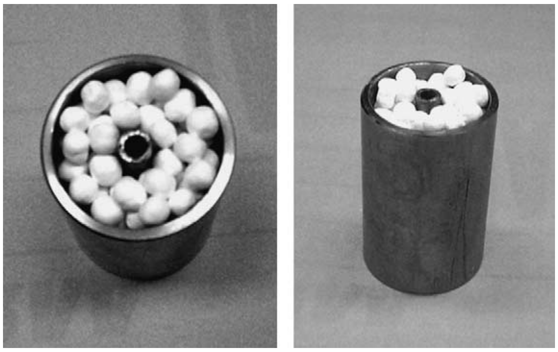

Fig. 4. Reactor tube load using the alumina support as an example.

with portable thermocouples inserted inside. Fig. 4 is the reactor tube loaded with the alumina support to be used for the catalyst preparation.

The reactor tube was mounted into a thermostat to remove the reaction heat. The thermostat was a vessel with a fluidized alumina bed used as a cooling agent. Air was supplied to the fluidized bed through a heating column. The temperature of the heat carrier was varied between 240 and 320 °C during experiments. The estimated coefficient of heat transfer between the fluidized bed and the vertical reactor tube was close to that between the tube and a salt melt commonly used as the cooling agent in tubular reactors.

The gas feeding system consisted of a unit for air and nitrogen supply, a water supply system and a unit for ammonia supply with a cylinder installed into the hot water thermostat. Each unit was equipped with an electric heating column. A chromatograph Zvet-500 with a heat conductivity detector was used for identification of components of the inlet and outlet gas mixtures, a NaX column being used for $O_2$ and $N_2$, and a Chromosorb-104 column for $NH_3$, $N_2O$ and $H_2O$. Outlet concentrations of NO and $NO_2$ were determined using a sensor gas analyzer Quintox.

### 5.2. Spherical catalysts

The appropriate catalyst activity for pilot reactor was found by modeling and the studies were carried out to develop the preparation procedure of catalyst pilot batches with optimal activity. Pilot testing was performed with two catalyst batches A and B. These batches were prepared with equal Mn/Bi content using the alumina support from the same box. Catalyst A was prepared by impregnation of 3–5 mm alumina spheres with the solution of manganese and bismuth nitrates followed by drying and calcination. Catalyst B was prepared using 5–6 mm alumina spherical granules by the same procedure except calcination conditions.

As it was noted earlier 0.25–0.5 mm fractions of crushed catalyst was used for measuring catalyst activity. The intrinsic activity of catalyst B was one third of that of catalyst A. The absence of intraparticle diffusion was confirmed evaluating the effectiveness factor for these fractions (see more detailed description in Appendix A).

### 5.3. Adjustment of operation regimes

To start up the reactor, the fluidized bed in the thermostat was heated to 245–250 °C and all columns to appropriate temperatures and the air/steam mixture was started feeding to the tubular reactor. As soon as the inlet wet air reached a constant temperature, ammonia was fed at a low rate to avoid the catalyst overheating. The process was initiated (the hot spot appeared) and the stable temperature regime was set in. The thermocouple was moved along the thermocouple tube to measure the temperature profile in 10 cm intervals.

Measurement of temperature profiles allowed the time for attainment of the steady-state to be determined. It was 1.5–3 h from the starting point of ammonia feeding to the reactor. The ammonia concentration was 3.0–5.0 vol.%, a stable hot spot was observed in the catalyst bed.

### 5.4. Influence of operation conditions

As mentioned earlier, the reactor parameters and the range of conditions for pilot testing were determined in terms of mathematical modeling (Table 2). The catalyst loading, catalyst activity, catalyst particle diameter, inlet ammonia and water concentrations, superficial gas velocity, inlet gas and cooling agent temperatures were varied in the course of pilot studies.

The influence of reactor parameters on the operation mode was studied with both catalysts A and B loaded into the reactor. With catalyst A, the experimental temperature profiles were more sensitive to the variable parameters due to its higher activity. The comparative data on sensitivity of the hot spot temperature to the inlet ammonia concentration are shown in Table 3 for both catalysts.

Less sensitive hot spot temperature profiles were observed with catalyst B. In this case, the operation regimes met the restrictions 1–3 and were easier controlled even though the thermostat temperature was higher (cf. runs 1–2 and 3–4 of Table 3). For this reason catalyst B was mainly used for experimental studies.

To maximize the inlet ammonia concentration, a series of experiments were run to choose the optimal inlet gas temperature, gas velocity, inlet water concentration and thermostat

Table 3
Effect of inlet $NH_3$ concentration on hot spot temperature

| Catalyst batch | A | A | B | B |
|---|---|---|---|---|
| Run number | 1 | 2 | 3 | 4 |
| Inlet gas temperature (°C) | 199 | 200 | 225 | 226 |
| Thermostat temperature (°C) | 256 | 257 | 306 | 309 |
| Inlet $H_2O$ concentration (vol.%) | 19.8 | 19.7 | 16.6 | 16.5 |
| Inlet $NH_3$ concentration (vol.%) | 4.0 | 4.3 | 3.6 | 4.0 |
| Hot spot temperature (°C) | 407 | 480 | 372 | 390 |

Table 4
Effect of inlet water and thermostat temperature

| Run number | 1 | 2 | 3 | 4 | 5 |
|---|---|---|---|---|---|
| Inlet $NH_3$ concentration (vol.%) | 3.5 | 3.6 | 3.7 | 3.5 | 3.6 |
| Inlet $H_2O$ concentration (vol.%) | 2.2 | 11 | 16.6 | 15 | 19.0 |
| Thermostat temperature (°C) | 299 | 304 | 306 | 310 | 312 |
| Hot spot temperature (°C) | 387 | 372 | 372 | 395 | 405 |
| $N_2O$ selectivity (%) | 86.8 | 85.6 | 85.2 | 86.8 | 88 |

temperature. The results obtained by modeling, viz. the minor dependence of the hot spot temperature on the inlet gas temperature, were experimentally supported. A significant influence of variations in the inlet water concentration and of the thermostat temperature on the hot spot temperature was observed. Table 4 shows examples of these experimental data. A wide range of variations of the gas velocity was not allowed due to a considerable increase in the pressure drop with an increase in the flow rate.

One can see from the data of Table 4 that an increase in the inlet water concentration results in lowering the hot spot temperature due to a decrease in the catalyst activity (cf. runs 1–3 in Table 4). Smoothed temperature profiles were observed at high water concentrations. Kinetic studies also showed a decrease in the activity at an increase in the water concentration (see Appendix A).

The influence of the thermostat temperature is illustrated in Table 4 and in Fig. 5. Elevation of the cooling agent temperature at close water concentrations results in an increase in the hot spot temperature (runs 3–5, Table 4). The stable steady-state temperature regimes can be provided by controlling the thermostat temperature at the hot spot temperature lower than 400 °C (Fig. 5) and the inlet ammonia concentration equal to 4.5–5%. Operation regimes achieved at low water concentrations also fitted the restrictions for these ammonia concentrations.

### *5.5. Comparative experimental and modeling data*

Experimental temperature profiles were compared to the profiles calculated in terms of the mathematical model. Modeling of temperature profiles in the pilot reactor was based on the data obtained by special experiments aimed at more precise determination of mass and heat transfer parameters, $D_r$, $\lambda_r$ and $\alpha_w$ according to the Eq. (3). The experimental temperature profiles were measured without reaction by feeding reaction mixture without ammonia, air and wet air to the pilot tube with the catalyst-loaded therein. Comparison of measured and calculated points allowed the best fitting to be found correcting the constant parameters of the Eq. (3).

The next step was modeling of operation regimes of the reactor at feeding the reaction mixture. The axial temperature profiles were calculated for the cases of low and high inlet water concentrations. The reaction rate constants were corrected for the high water concentration in terms of the data of kinetic studies (see Appendix A). The simulated data agreed well enough with the experimental points, the difference between them being no more than 15 °C for all experimental temperature profiles. The comparative results are exemplified in Fig. 6.

Thus, rather simple mathematical model (2) was demonstrated to be appropriate for simulation of the operation regimes. This description can be used for optimization of

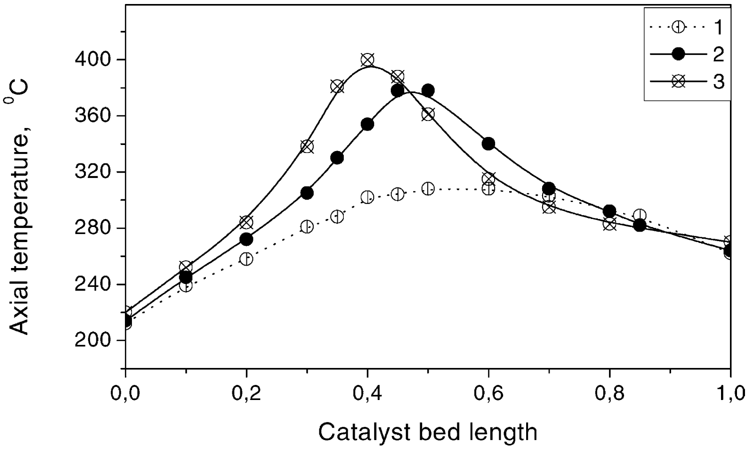

Fig. 5. Temperature profiles along the reactor axis at various thermostat temperature. Inlet water concentration: 15–20%; superficial gas velocity: 3 m/s. Thermostat temperature: (1) 265 °C; (2) 260 °C; (3) 250 °C.

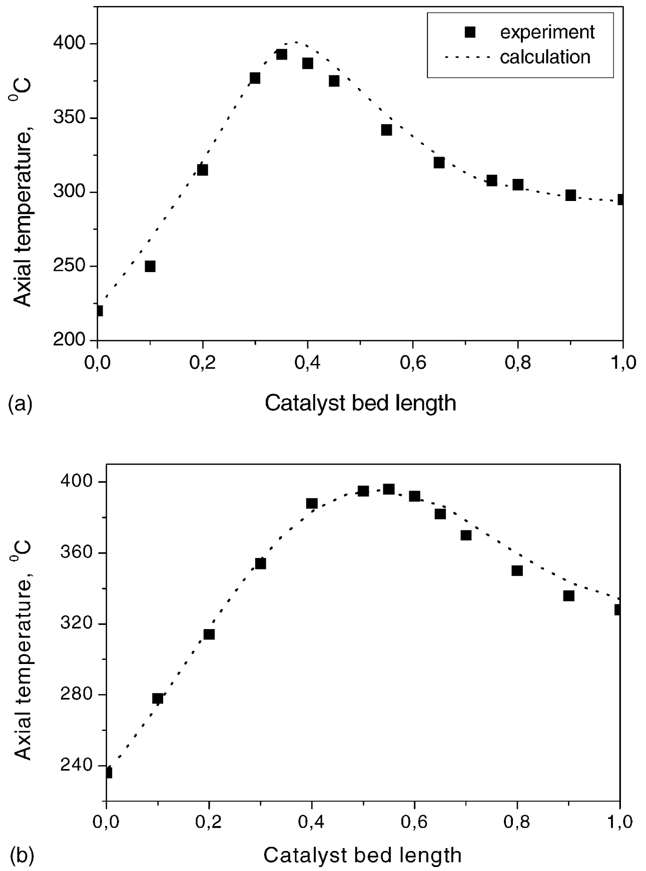

Fig. 6. Comparison of measured and calculated temperature profiles for low (a) and high (b) water concentrations. Inlet ammonia concentration: 4.0%; superficial velocity: 3 m/s; inlet water concentration: (a) 2.2%, (b) 15%.

parameters of the tubular reactor and for prediction of the technological regimes. The ammonia conversion and, consequently, the temperature profiles of the real reactor can be evaluated based on the first-order kinetic equations of formation of nitrous oxide and nitrogen (see Appendix A). The kinetic model needs further improvement for more exact estimation of the selectivity to $N_2O$.

### 5.6. *Principal results of pilot testing*

Here is a summary of results obtained by experimental studies and simulation:

- Ammonia oxidation into nitrous oxide was realized in a pilot single-tube cooling reactor with Mn/Bi/Al spherical catalyst based on the data of kinetic studies and reactor modeling.
- Stable and easily controlled temperature regimes were obtained at the inlet ammonia concentration of 4–5%.
- For almost 100% ammonia conversion the 87–88% selectivity to nitrous oxide is achieved, selectivity to nitrogen oxide being not higher than 0.5%.
- Modeling of pilot reactor demonstrated a good agreement (at the accuracy of 15 °C) between experimental and calculated temperature profiles.
- Adequacy of the mathematical model was confirmed. Hence, this model can be used for prediction of technological regimes.

Table 5
Main process characteristics for $N_2O$ synthesis in a tubular reactor

| | Spherical catalyst | Rashig ring catalyst |
|---|---|---|
| Maximum dimension (mm) | 5–6 | 7 × 7 × 2 |
| Inlet ammonia concentration (%) | 4–5 | 7–8 |
| Theoretical adiabatic temperature rise (°C) | 300–400 | 550–650 |
| Catalyst productivity (ton $N_2O$ per ton catalyst par day) | 4.0–4.5 | 5.0–5.5 |

## 6. Conclusions

Pilot testing of the process of ammonia oxidation by air oxygen was performed with a single-tube reactor as the model of a unit of the real industrial multi-tubular reactor. Spherical Mn/Bi/Al catalyst was loaded in the pilot reactor. The results obtained with the developed catalyst show the feasibility of the process for catalytic synthesis of nitrous oxide from ammonia in a tubular reactor to provide a high selectivity towards nitrous oxide and stable catalyst operation.

The experimental efforts were guided by the modeling results. The good agreement between the experimental and calculated data assures that the proposed mathematical description is appropriate for prediction of the technological operation regimes and for optimization of the industrial multi-tubular reactor. More confident prediction of the selectivity to nitrous oxide needs further studies to develop the kinetic model.

The operation regimes in the ring catalyst-loaded tubular reactor were modeled to determine characteristics of the industrial reactor. The results obtained show that the process can be achieved at the inlet ammonia concentration of ca. 7–8%. Sufficiently stable operation regimes at high inlet ammonia concentrations are expected with Rashig rings packed in the tubular reactor. For the conditions under study, the hot spot temperature is not higher than 380–390 °C. Thus, 140–160 °C temperature rise above the inlet temperature is observed in the tubular reactor, whereas the theoretical adiabatic temperature rise is 550–650° (Table 5).

## Acknowledgements

The authors are gratefully acknowledged to the Solutia Incorporated for financial support of these studies.

## Appendix A

Rate $W$ of ammonia oxidation was calculated as

$$W = W_{\mathrm{kin}}\eta,$$

where $W_{\mathrm{kin}}$ was the intrinsic reaction rate for fine particles and $\eta$ the catalyst effectiveness factor. According to Eq. (1) the intrinsic reaction rate was expressed as:

$$W_{\mathrm{kin}} = 2W_{\mathrm{N_2O}} + 2W_{\mathrm{N_2}} + W_{\mathrm{NO}}$$

Catalyst activity and selectivity was shown in part 3 to depend on oxygen and water concentrations in wide range. However, it was possible to choose the conditions with high nitrous oxide selectivity where such dependences were slight and the rates of nitrous oxide and nitrogen formation were fit to first-order equations with satisfied accuracy for these separate regions. It was assumed for modeling that

$$W_{\mathrm{N_2O}} = k_1C, \quad W_{\mathrm{N_2}} = k_2C$$

and selectivity to nitrous oxide was constant for oxygen excess, low and high water concentrations. The formation rate of nitrogen oxide $W_{\mathrm{NO}}$ was taken to be equal zero due to low nitrogen oxide concentrations obtained in kinetic studies.

Constants $k_1$ and $k_2$ and the corresponding activation energies were determined from kinetic data. Reaction rate for modeling with high water concentrations was determined as $W = W_{\mathrm{kin}}\eta a$, where $a$ is activity coefficient. This value was calculated as the relation of sum of constants $k_1$ and $k_2$ for low water concentrations to one for high water concentrations.

Effectiveness factor $\eta$ was evaluated calculating the Thiele modulus for first-order reaction rate and comparing it with literature data [10]. Binary diffusivities do not differ considerably, so the Thiele modulus was calculated with the averaged diffusivity:

- The influence of intraparticle diffusion was absent for crushed catalyst of fraction 0.25–0.5 mm.
- Effectiveness factor for pilot batches was estimated for different temperatures and it was assumed to be constant for modeling of pilot regimes.

Reaction heat release is calculated as $Q = Q_1S + Q_2(1-S)$, where $Q_1$ and $Q_2$ are heat effects for nitrous oxide and nitrogen formation rates (1), respectively and $S$ is the selectivity to nitrous oxide calculated as $S = k_1/(k_1 + k_2)$. Fortunately, heat released during formation of nitrous oxide and nitrogen do not differ considerably. Therefore, the earlier simplifications have a minor effect on the total release of heat.

## References

[1] A.K. Uriarte, M.A. Rodkin, M.J. Gross, A.S. Kharitonov, G.I. Panov, in: R.K. Grasselli, S.T. Oyama, A.M. Gaffney, J.E. Lyons (Eds.), Proceedings of the 3rd International Congress on Oxidation Catalysis, Elsevier, Amsterdam, Stud. Surf. Sci. Catal. 110 (1997) 857–864.
[2] G.I. Panov, A.K. Uriarte, M.A. Rodkin, V.I. Sobolev, Catal. Today 41 (1998) 365–385.
[3] A.K. Uriarte, in: A. Corna, F.V. Melo, S.Mendioroz, J.L.G. Fierro (Eds.), Proceedings of the 12th International Congress on Catalysis, Elsevier, Amsterdam, Stud. Surf. Sci. Catal. 130 (2000) 743–748.
[4] Jpn. Chem. Week 35(1758) (1994) 9.
[5] Japanese Patent 5-139710, 1993.
[6] Japanese Patent 6-122505, 1994; 6-122506, 1994; 6-122507, 1994.
[7] I. Zawadski, Discuss. Faraday Soc. 8 (1950) 140–152.
[8] V.V. Mokrinsii, E.M. Slavinskaya, A.S. Noskov, I.A. Zolotarsky, PCT Int. Appl. WO 9825698 (1998), priority: RU 96-96123343.
[9] N.I. Il'chenko, G.I. Golodets, J. Catal. 39 (1975) 57–86.
[10] G.F. Froment, K.B. Bischoff, Chemical Reactor Analysis and Design, Wiley, New York, USA, 1979.
[11] M.E. Aerov, O.M. Todes, Reactors with stationary granular bed, Chemistry, Khimia, Leningrad, 1979.